

## SYNTHESIS AND SENSING CHARACTERISTICS OF AB-TYPE BLOCK COPOLYMERS WITH FLUORESCENT PROBE

VIOLETA MELINTE\*, TINCA BURUIANA, ANDREEA CHIBAC, EMIL C. BURUIANA

*Petru Poni Institute of Macromolecular Chemistry, 41 A Gr. Ghica Voda Alley, 700487 Iasi, Romania*

This article reports the synthesis through atom transfer radical polymerization (ATRP) of fluorescent block copolymers using the poly(ethylene oxide) containing terminal bromine atom as macroinitiator and hydrophilic block, while the hydrophobic block consists of *n*-butyl methacrylate and 2-methacryloyloxyethylcarbamoyloxymethylpyrene taken in various molar ratios. The characterization of the polymers was achieved by Fourier-transform infrared spectroscopy (FTIR), <sup>1</sup>H-nuclear magnetic resonance (<sup>1</sup>H NMR), gel permeation chromatography (GPC), differential scanning calorimetry (DSC), thermogravimetric analysis and atomic force microscopy (AFM). Thus, the molecular weight and the molar composition of the block copolymers were estimated by <sup>1</sup>H NMR spectrometry, and were further confirmed by GPC analysis. Additionally, the fluorescence response of the pyrene-containing block copolymers towards certain metal ions (Pb<sup>2+</sup>, Co<sup>2+</sup>, Hg<sup>2+</sup>, Ni<sup>2+</sup>, UO<sub>2</sub><sup>2+</sup>, Zn<sup>2+</sup>), nitromethane and iodide anions in water was investigated, the study demonstrating that the synthesized block copolymers are viable candidates as fluorescent receptors for uranyl ions that can discriminate low concentrations of UO<sub>2</sub><sup>2+</sup>. The significant effect of iodide ions on the fluorescence intensity of the block copolymers in solution or in film state could be exploited in the development of 'turn-off' or 'turn-on' chemosensors for this type of analyte.

(Received January 9, 2012; Accepted March 27, 2012)

*Keywords:* block copolymer, ATRP polymerization, fluorescence quenching

### 1. Introduction

Block copolymers consisting of two or more blocks of different nature and covalently attached, usually lead to interesting physicochemical properties of the resulted materials [1, 2]. In particular, amphiphilic block copolymers are recognized for their ability to exhibit a complex self-assembling behaviour when they are dissolved into a selective solvent for one block, creating thus the possibility to spontaneously segregate in well-defined special morphologies, which can improve their properties and can guide, in proper conditions the formation of nanoparticles, nanoshells or nanotubes used in top biomedical fields [3, 4]. Until now, numerous studies have been devoted to the synthesis and characterization of biocompatible polymers based on poly(ethylene oxide), given its excellent water solubility, chain mobility, and non-immunogenicity, so that in combination with various hydrophobic structures (poly(amino acid), poly(meth)acrylates, polycaprolactone) provided complex macromolecular architectures [5-8].

On the other hand, an important aspect concerning the synthesis of a variety of amphiphilic block copolymers with controlled structure that can self-assemble in aqueous solution is associated with the recent development in living/controlled radical polymerization methods. Hence, techniques such as atom transfer radical polymerization (ATRP) [9], reversible additional fragmentation chain transfer (RAFT) [10], nitroxide-mediated polymerization (NMP) [11] and single-electron-transfer living radical polymerization (SET-LRP) [12], or combinations of them

---

\*Corresponding author: viomel@icmpp.ro

[13-15] manifest many positive features, including the ability to control the composition and molecular weight of the block copolymers prepared through such methodologies. Over time, since its discovery by both Matyjaszewski and Sawamoto in 1995 [16, 17], ATRP proved to be an efficient route for the synthesis of polymers with designed structures in a controlled manner [18, 19], especially using the Cu-based catalytic system and a large range of functional initiators [20]. Thus, it has been successfully employed in the obtaining of tailored block copolymers, like block and graft copolymers, star polymers, hyperbranched polymers, and dendrimers based on all type of acrylate or methacrylate monomers [21].

Modern research actively investigates the chemosensors field in order to extend innovative devices that convert the molecular recognition into highly sensitive and easily detected signals. Accordingly, numerous chemosensors for metal ions were described as being able to correlate metal ions concentration with changes in spectroscopic characteristics of the analyzed samples [22, 23]. Recognized for their spectroscopic properties of large molar extinction coefficient and high fluorescence quantum yield, pyrene derivatives are excellent candidates for the design of some sensors with high sensitivity [24]. Moreover, the physical/covalent attachment of fluorescent molecules to polymer samples has been advantageously explored for the generation of fluorescent nanostructures used in molecular imaging [25, 26].

Taking advantage of these findings, the present paper is focused on the synthesis via atom transfer radical polymerization of new amphiphilic block copolymers based on poly(ethylene glycol) hydrophilic component and hydrophobic n-butyl methacrylate, in which pyrene units are covalently included on the hydrophobic segment. The structural characterization of the block copolymers was achieved through specific methods ( $^1\text{H}$  NMR, FTIR, TGA, DSC), whereas the fluorescence response of pyrene fluorophore in the presence of various heavy metal cations, nitromethane or potassium iodide has been investigated.

## 2. Experimental

### 2.1. Materials

Poly(ethylene glycol) methyl ether ( $M_w = 2000$ ), 2-bromoisobutyryl bromide, triethylamine, 1-pyrene methanol, 2-isocyanatoethyl methacrylate, n-butyl methacrylate (BMA), CuBr, *N,N,N',N'',N'''*-pentamethyldiethylenetriamine (PMDETA), were purchased from Sigma Aldrich Chemical Co. and used without further purification. Potassium iodide (KI), nitromethane, lead (II) acetate trihydrate, cobalt (II) acetate tetrahydrate, mercury (II) acetate, nickel (II) acetate tetrahydrate, uranyl acetate dihydrate, zinc acetate dihydrate were purchased from Sigma Aldrich Chemical Co. and used without further purification.

### 2.2. Synthesis of the PEO macroinitiator

The preparation of the macroinitiator based on poly(ethylene oxide) that contains bromine atom (PEO-Br) was performed accordingly to procedure previously reported [27]: into a three-neck round-bottom flask equipped with condenser, dropping funnel, gas inlet/outlet, and a magnetic stirrer 0.7 mL (5 mmol) triethylamine in 10 mL of dry  $\text{CH}_2\text{Cl}_2$  were cooled to 0 °C and 0.64 mL (5 mmol) 2-bromoisobutyryl bromide in 10 mL  $\text{CH}_2\text{Cl}_2$  were added. To the resulting mixture, 10 g (5 mmol) PEG methyl ether ( $M_w = 2000$ ) dissolved in 25 mL methylene chloride were dropwise added at such a rate that the reaction temperature was maintained at 0 °C. Then, the temperature was risen to room temperature and the mixture was kept under stirring for 24 h. The solution was filtered, evaporated to half and the PEO-Br derivative was obtained by precipitation in cold diethyl ether and dried under vacuum. Yield 8.9 g (83 %).

$^1\text{H}$  NMR ( $\text{CDCl}_3$ ,  $\delta$  ppm): 3.64 (m, 180H, O- $\text{CH}_2$ - $\text{CH}_2$ -O); 3.38 (s, 3H,  $\text{CH}_3$ -O- $\text{CH}_2$ -); 1.93 (s, 6H,  $\text{CH}_3$ -C-Br). FTIR (KBr,  $\text{cm}^{-1}$ ): 2872 (C-H); 1735 (C=O); 1112 (C-O-C); 531 (C-Br).

### 2.3. Synthesis of 2-methacryloyloxyethylcarbamoyloxymethylpyrene (MAPy)

To a solution of 1-pyrene methanol (3 g, 13 mmol) in methylene chloride, 1.86 mL (13 mmol) 2-isocyanatoethyl methacrylate was dropwise added in the presence of dibutyltindilaurate used as catalyst. The reaction mixture was stirred at 40 °C for 24 h under a nitrogen atmosphere, the course of the reaction being followed through the infrared absorption of the isocyanate

stretching band ( $2260\text{ cm}^{-1}$ ). The urethane resulting product (MAPy) was collected after removing the solvent under vacuum as yellow powder. Yield 4.6 g (92 %).

$^1\text{H NMR}$  ( $\text{DMSO-d}_6$ ,  $\delta$  ppm): 8.5-8 (m, 9H, aromatic); 7.5 (t, 1H, NH); 6.05 (s, 1H,  $\text{CH}_2=\text{C}$  in trans position relative to  $\text{CH}_3$  unit); 5.79 (s, 2H,  $\text{NH-COO-CH}_2$ ); 5.63 (s, 1H,  $\text{CH}_2=\text{C}$  in cis position relative to  $\text{CH}_3$  unit); 4.12 (m, 2H,  $\text{COO-CH}_2\text{-CH}_2\text{-NH}$ ); 3.36 (m, 2H,  $\text{COO-CH}_2\text{-CH}_2\text{-NH}$ ); 1.84 (s, 3H,  $\text{CH}_2=\text{C-CH}_3$ ). FTIR (KBr,  $\text{cm}^{-1}$ ): 3301 (NH); 2854-2956 (C-H); 1718 (CO); 1687 (amide I); 1636 and 817 ( $\text{CH}=\text{C}$ -); 1549 (amide II); 1274 and 1174 (C-O).

#### 2.4. Synthesis of the block copolymers

In the preparation of block copolymers, PEO-Br was used as ATRP macroinitiator. Into a typical experiment, 2 g (0.93 mmol) macroinitiator, 0.133 g (0.93 mmol) CuBr and 0.45 mL (2.139 mmol) PMDETA (with molar ratios initiator:CuBr:PMDETA = 1:1:2.3) were dissolved in 5 mL dioxane. The solution was deoxygenated by freeze-pump-thaw cycles, followed by the addition of 13 g (91.2 mmol) n-butyl methacrylate and 0.72 g (1.86 mmol) MAPy. The polymerization was performed into a flame-sealed glass ampoule at  $80\text{ }^\circ\text{C}$ , under argon for 48 h. After this time, the polymerization was terminated by exposure to air and dilution with THF. Polymerization solution was then purified on alumina columns to remove copper catalyst. The excess solvent was removed by rotary evaporation and the solid product was recovered after precipitation in methanol and drying in vacuum at  $40\text{ }^\circ\text{C}$  overnight.

The second block copolymer (COP-B2) was similarly prepared, the initial molar ratio of the partners being of PEO-Br:CuBr:PMDETA:BMA:MAPy = 1:1:2.3:490:10. Applying the same purification method, COP-B2 block copolymer was obtained with a yield of 80.6 %.

**COP-B1:** GPC:  $M_w = 16900$ ,  $M_w/M_n = 1.12$ . FTIR (KBr,  $\text{cm}^{-1}$ ): 3432 (NH); 2874-2959 (C-H); 1728 (CO); 1242 and 1147 (C-O).

**COP-B2:** GPC:  $M_w = 65000$ ,  $M_w/M_n = 1.29$ .  $^1\text{H NMR}$  ( $\text{CDCl}_3$ ,  $\delta$  ppm): 8.4-8 (m, 72H, aromatic); 5.86 (s, 4H,  $\text{NH-COO-CH}_2$ ); 3.94 (m, 790H,  $\text{COO-CH}_2\text{-CH}_2$ ); 3.64 (m, 181H,  $\text{O-CH}_2\text{-CH}_2\text{-O}$ ); 3.38 (s, 3H,  $\text{CH}_3\text{-O-CH}_2\text{-CH}_2$ ); 2.1-1.3 (m, 2386H,  $\text{COO-CH}_2\text{-CH}_2\text{-CH}_2\text{-CH}_3$  and  $-\text{CH}_2\text{-C}(\text{CH}_3)\text{-COO}$ ); 1.15-0.80 (m, 2394H,  $\text{CH}_2\text{-CH}_2\text{-CH}_3$  and  $-\text{CH}_2\text{-C}(\text{CH}_3)\text{-COO}$ ). FTIR (KBr,  $\text{cm}^{-1}$ ): 3432 (NH); 2875-2959 (C-H); 1728 (CO); 1242 and 1147 (C-O).

#### 2.5. Instrumentation and measurements

The structures of the monomer, macroinitiator and block copolymers were verified by  $^1\text{H NMR}$  spectrometry and FTIR spectroscopy using a Bruker Avance DRX 400 spectrometer and a Bruker Vertex 70 FT-IR instrument, respectively. Gel permeation chromatography (GPC) measurements were carried out using an equipment supplied by Polymer Laboratories Ltd., at room temperature with a single PL-Mixed "D" column (bead size  $5\text{ }\mu\text{m}$ ; pore sizes = 100, 500,  $10^3$ ,  $10^4\text{ }\text{\AA}$ ). The mobile phase was THF (containing 2% triethylamine), delivered at a flow rate of  $1\text{ mL min}^{-1}$  using a Waters 515 isocratic pump. The refractive index was measured with an ERC-7515A refractive index detector also supplied by Polymer Laboratories Ltd. The instrumentation was calibrated using low polydispersity poly(methyl methacrylate) (PMMA) standards supplied by Polymer Laboratories Ltd. The thermal stability of the PEO-Br and block copolymers was analyzed through thermogravimetry using a MOM Budapest derivatograph. TG and TGA curves were recorded between 20 and  $600\text{ }^\circ\text{C}$  with a heating rate of  $12\text{ }^\circ\text{C}\cdot\text{min}^{-1}$  in air. The thermal transitions temperatures were determined using a differential scanning calorimeter (Pyris Diamond DSC, Perkin Elmer USA). For analysis, 10-15 mg of the samples were placed in an aluminium pan. They were scanned from  $-100$  to  $+150\text{ }^\circ\text{C}$  and subsequently cooled to  $-100\text{ }^\circ\text{C}$  at a rate of  $20\text{ }^\circ\text{C min}^{-1}$ , kept for 5 min at  $-100\text{ }^\circ\text{C}$ , and finally reheated to  $150\text{ }^\circ\text{C}$  with the same rate. The glass transition temperature ( $T_g$ ) was evaluated as the midpoint temperature of the characteristic heat capacity change detected in the second heating traces. Polymer surface morphology was examined by atomic force microscopic (AFM) technique using a SOLVER PRO-M AFM. The polymeric films for AFM experiment were prepared using a spin coater Model WS-400B-6NPP/LITE/10K from Laurel Tech at 3000 rpm, the images being registered in different points of the sample to check their reproducibility. The fluorescence intensity measurements were done on a Perkin-Elmer

LS 55 spectrophotometer at room temperature in water, dimethylformamide, THF and chloroform (without corrections). The influence of various analytes (metal cations, iodide ions or nitromethane) on the fluorescence spectra of the block copolymers was examined by adding different volume of analyte stock to a known volume of the polymer solution (4 mL) and stirring to equilibrium. Excitation was carried at  $\lambda_{\text{ex}} = 320$  nm, whereas the emission spectra were recorded in the range of 330 - 600 nm.

### 3. Results and discussion

#### 3.1 Design and characterization of the block copolymers

For the preparation of poly(ethylene oxide)-*b*-poly(*n*-butyl methacrylate-*co*-2-methacryloyloxyethylcarbamoyloxymethylpyrene) block copolymers (COP-B1 and COP-B2) by atom-transfer radical polymerization, the reaction of poly(ethylene glycol) methyl ether with 2-bromoisobutyryl bromide was firstly performed in order to obtain the macroinitiator end-capped with bromine atom (PEO-Br) [27]. Furthermore, the synthesis of new fluorescent block copolymers assumed firstly the preparation of an appropriate pyrene derivative with methacrylic polymerizable moiety (MAPy), using a conventional addition reaction of 1-pyrene methanol to 2-isocyanatoethylmethacrylate. The structure of the formed monomer 2-methacryloyloxyethylcarbamoyloxymethyl pyrene was confirmed by spectroscopic techniques, its  $^1\text{H}$  NMR spectrum being displayed in Figure 1.

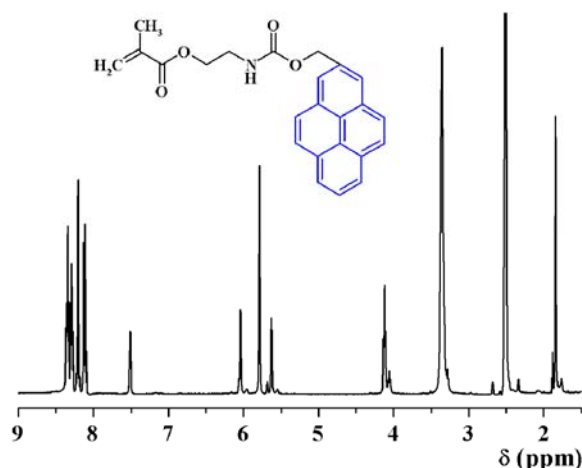
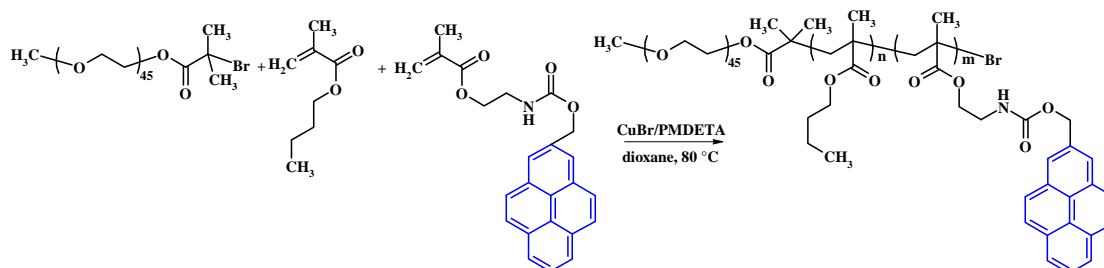


Fig. 1. Chemical structure and the  $^1\text{H}$  NMR spectrum of MAPy in  $\text{DMSO-}d_6$ .

For the synthesis of the block copolymers (outlined in Scheme 1), the PEO-Br macroinitiator was used together with a mixture of methacrylic monomers (*n*-butyl methacrylate and 2-methacryloyloxyethylcarbamoyloxymethyl pyrene) in various molar ratios, adjusting the feed ratio of monomers to macroinitiator (the detailed polymerization conditions are listed in Table 1).

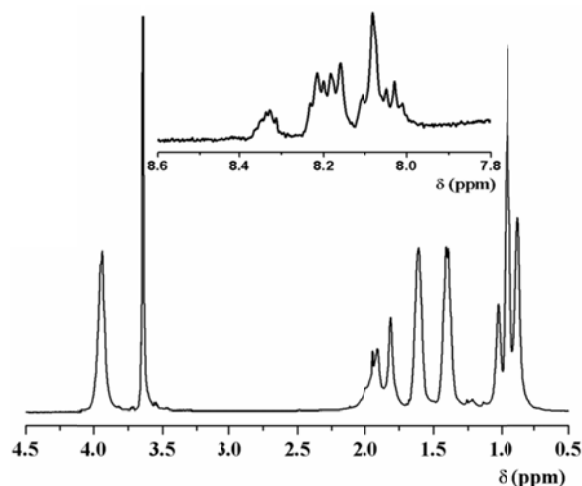


Scheme 1. Reaction scheme for the synthesis of block copolymers COP-B1 and COP-B2

Table 1. Experimental conditions and properties of block copolymers prepared by ATRP

Sample	PEO-Br:CuBr:PMDETA: BMA:MAPy	Conversion (%)	$M_{n,NMR}$	$M_{w,GPC}$	$M_w/M_n$
COP-B1	1:1:2.3:98:2	86.73	14600	16900	1.12
COP-B2	1:1:2.3:490:10	80.61	61300	65000	1.29

The proposed structures of the macroinitiator and block copolymers were confirmed by spectral methods ( $^1\text{H}$  NMR spectrometry and FTIR spectroscopy). The  $^1\text{H}$  NMR study on COP-B1 block copolymer (Figure 2) reveals the appearance of the peaks corresponding to the aromatic protons from pyrene molecule between 8.4 and 8 ppm, while the signal at 5.86 ppm is assigned to the methylene protons located between the pyrene unit and the urethane-ester group. The signal from 3.94 ppm corresponds to the methylene protons coming from the butyl methacrylate units linked to the ester function, and the intense peak at 3.64 ppm can be attributed to the protons of the methylene units from the PEO macroinitiator, whereas the singlet at 3.38 ppm is given by the protons of the methyl ester group from PEO. The methylene protons from butyl methacrylate and the methylene protons from the macromolecular backbone give signals in the region 2.0-1.4 ppm, while the peaks in the region 1.03-0.87 ppm belong to the methyl protons originating from the same sequences. From the integration of the peak areas for aromatic protons (8.4-8 ppm), methylene protons from n-butyl methacrylate in the neighbourhood of ester units (3.94 ppm) and the methylene protons from the PEO sequences (3.64 ppm) observed in the  $^1\text{H}$  NMR spectrum of COP-B1 block copolymer, the copolymer composition was calculated as being of 1:85:1 (PEO:BMA:MAPy), corresponding to a molecular weight  $M_{n,HNMR}$  of 14600. Likewise, applying the same algorithm in the case of COP-B2, the structural composition calculated from the  $^1\text{H}$  NMR spectrum corresponds to a value of 1:395:8 (PEO:BMA:MAPy) and a molecular weight  $M_{n,HNMR}$  of 61300.

Fig. 2.  $^1\text{H}$  NMR spectrum of COP-B1 block copolymer in  $\text{CDCl}_3$ .

The molecular weight ( $M_w$ ) and polydispersity index measurements for the synthesized block copolymers was determined by gel permeation chromatography (GPC) using tetrahydrofuran as the eluent. The values of the  $M_w$  reported in Table 1 indicated that the copolymers possess relatively high molecular weights (COP-B1: 16.9 kDa; COP-B2: 65 kDa), comparable with those calculated from the  $^1\text{H}$  NMR spectra. Moreover, the polydispersity indexes of the block copolymers ( $\text{PDI}_{\text{COP-B1}} = 1.12$  and  $\text{PDI}_{\text{COP-B2}} = 1.29$ ) are relatively narrow, a characteristic for ATRP processes [20]. The pure block copolymers are soluble in common organic solvents (chloroform, THF, DMF, DMSO), and by solution casting they give homogeneous films with a good adhesion on a variety of substrates and high optical quality.

### 3.2. Thermal properties and surface characteristics

To assess the thermal properties for the block copolymers, thermogravimetric analysis (TGA) and differential scanning calorimetry (DSC) were carried out, the obtained results being included in Table 2.

Table 2. Thermal properties of the macroinitiator and block copolymers

Sample	$T_i$ (°C)	$T_f$ (°C)	$T_{10\%}$ (°C)	$T_{max}$ (°C)	Weight loss (%)	$T_g$ (°C)
PEO-Br	190	440	285	392	85.6	-
COP-B1	240	455	295	380	88.8	37.2
COP-B2	237	445	295	360	87.2	40.6

As can be observed, the decomposition process of the macroinitiator begins around 190 °C and is with about 50 °C lower than the onset of thermal degradation measured for the block copolymers, remark that suggests an enhanced thermal stability in the case of the block copolymers, attributed to the presence of poly(n-butyl methacrylate). The thermal degradation of the investigated polymeric materials occurred into a single step, in which most of the polymer chains are decomposed as estimated from the amount of residue. Concerning the thermal characterization of the block copolymers by DSC, the results included in Table 2 show that longer block length of poly(n-butyl methacrylate) in COP-B2 resulted in higher glass transition temperature ( $T_g$  at about 40.6 °C) as compared with COP-B1 ( $T_g$  at 37.2 °C), while the  $T_g$  for poly(ethylene oxide) in PEO-Br macroinitiator could not be detected probably due to the high crystallinity of the sample [28].

The surface morphology and topographic features of the block copolymers in thin films were examined by atomic force microscopy (AFM).

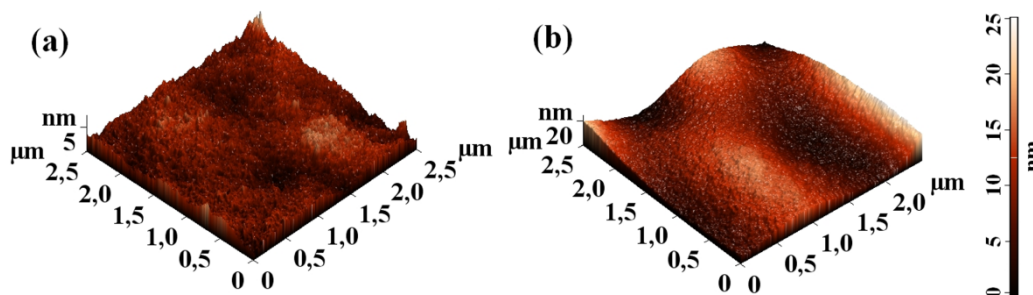


Fig. 3. 3D AFM images for polymeric films based on pyrene-containing block copolymers COP-B1 (a) and COP-B2 (b).

Fig. 3 shows the 3D morphological images of the block copolymers in thin films obtained by spin coating, where no important differences between the surface morphology of the films can be visualized. Thus, the surfaces of both copolymers appeared homogeneous and almost flat with small arrangements of several nanometers in height and with a measured root-mean-square surface roughness value ( $R_a$ ) of about 0.8 nm (COP-B1) and 4.1 nm respectively (COP-B2). The minor differences noticed in the surface morphology of the block copolymers are attributed principally to the small structural dissimilarities of these polymeric architectures, where the hydrophilic block has a length much smaller than the hydrophobic one, and the formation of nanostructured domains occurred in the same manner for both surfaces.

### 3.3. Optical properties

It is a well known issue that the pyrene fluorophore displays a very intensive fluorescence emission, having a high quantum yield and lifetime. Moreover, its fluorescence emission spectrum is very sensitive to solvent polarity due to the fact that its excited state has a different, non-planar structure than the ground state, reason for that pyrene probe has been widely used to precisely evaluate polymer/solvent microenvironments [29]. Until now, the literature data reported various applications of pyrene molecule in determining self-aggregation behaviour of block copolymers in an aqueous milieu, the pyrene being physically entrapped inside the aggregate or chemically attached to the macromolecular backbone, especially as polymerization initiator [30]. Also, due to its specific sensitivity, the pyrene fluorophore was often employed in the obtaining of chemosensors for the detection of ionic metals [31]. Therefore, as a continuation of our work concerning the synthesis of new photosensitive polymers useful in the development of sensors for metal cations [32, 33], here we describe some photophysical aspects concerning the interaction of pyrene molecules enclosed into the polymeric chain with different heavy metal ions, iodide ions or nitromethane.

From this perspective, the fluorescence spectra of the pyrene-labelled block copolymers were initially recorded in various solvents (water, DMF, THF and chloroform) keeping the same polymer concentration in solution and identical registration parameters. Thus, by excitation with  $\lambda_{\text{ex}} = 320$  nm, these materials emit a blue fluorescence with well-defined maxima characteristic for monomer fluorescence (375 - 425 nm) of pyrene (Figure 4). It may be observed that although the concentration of the measured solutions was constant ( $0.04 \text{ g L}^{-1}$ ), the intensity of fluorescence maxima for the block copolymers varies within broad limits, the higher fluorescence intensity being obtained for the copolymer solutions in water, whereas the lower absorption maxima were recorded in THF and chloroform. It can be assumed that in water, which is a good solvent for the hydrophilic PEG block, the polymer tend to form aggregates, where the molecular motion of pyrene is suppressed, determining the decrease of the thermal deactivation of the electronically excited state [34]. Additionally, in the case of COP-B1 block copolymer with lower molecular weight, the excimer fluorescence (470 nm) of pyrene is visible, suggesting that at this concentration, the micelles formation is remarked, situation that favour the inclusion of pyrene inside the hydrophobic block in tandem with the reducing of the distance between pyrene molecules [35].

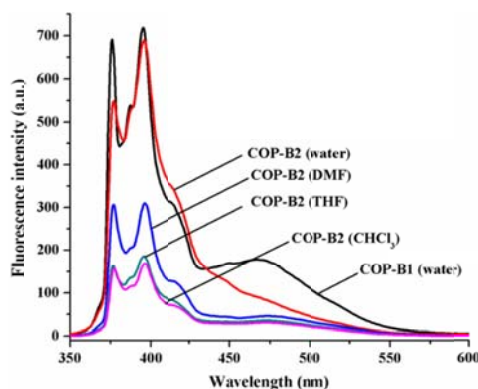


Fig. 4. Fluorescence spectra of pyrene-block copolymers ( $0.04 \text{ g L}^{-1}$ ) in various solvents.

The influence of various metal ions ( $\text{Pb}^{2+}$ ,  $\text{Co}^{2+}$ ,  $\text{Hg}^{2+}$ ,  $\text{Ni}^{2+}$ ,  $\text{UO}_2^{2+}$  and  $\text{Zn}^{2+}$ ) on the fluorescence intensity of the pyrene covalently linked to the COP-B2 was tested in aqueous solution. This study was triggered by the fact that the subject of heavy metal pollution has generated a great deal of concern in recent years, due to their inherently toxic effects on the environment and human health.  $\text{UO}_2^{2+}$  is one of the ions for which highly sensitive and selective sensors are necessary, owing to its importance in various physiological, medicinal and industrial processes, as well as in the nuclear industry, where is present in low quantities ( $10^{-5}$ - $10^{-3}$  M) in wash streams coming out of nuclear reactors both in aqueous as well as non-aqueous medium. Figure 5 (a) displays the fluorescence intensity changes for pyrene block copolymer COP-B2 excited at  $\lambda_{\text{ex}} = 320$  nm, in the presence of  $\text{UO}_2^{2+}$  cations. Hence, the fluorescence of pyrene is significantly quenched by the addition of  $\text{UO}_2^{2+}$  ions, the minimum detectable concentration of

uranyl cations being of  $5 \times 10^{-5}$  M, whereas the adding of 3 mM  $\text{UO}_2^{2+}$  produces a fluorescence quenching of about 85 %.

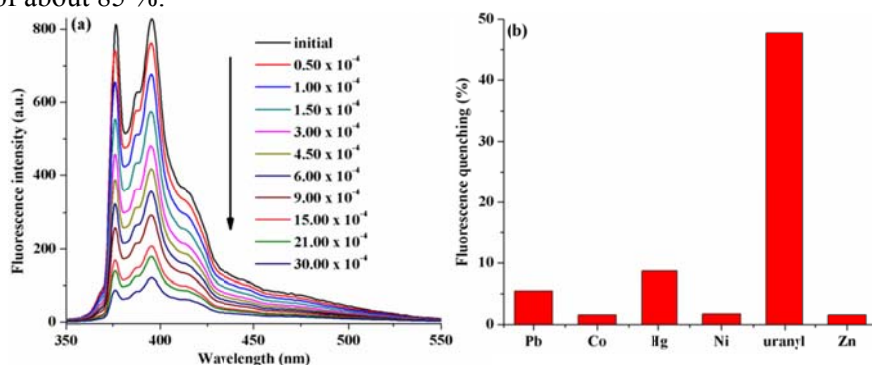


Fig. 5. Fluorescence spectral changes of aqueous solution of COP-B2 with different concentrations of  $\text{UO}_2^{2+}$  (a) and the fluorescence quenching degree (from  $I_0/I$  ratio) in the presence of various metal ions.

The fluorescence quenching efficiency measured from the  $I_0/I$  ratio, where  $I_0$  and  $I$  are the values of fluorescence intensities initially and in the presence of a quencher, was evaluated for all analytes at a concentration of  $4 \times 10^{-4}$  M (Figure 5, b). It may be noted that for  $\text{Pb}^{2+}$ ,  $\text{Co}^{2+}$ ,  $\text{Hg}^{2+}$ ,  $\text{Ni}^{2+}$  and  $\text{Zn}^{2+}$ , the fluorescence is quenched at rates between 1.5 to 8.7 %, while  $4 \times 10^{-4}$  M of uranyl cations induced a fluorescence quenching of 47.7 %. This experimental finding suggests that the considered system can be successfully employed in the selective detection of uranyl ions from aqueous environments at very low concentrations of quencher (in the range of  $10^{-5}$  M).

Considering that fluorescence quenching experiments can provide information concerning the degree of accessibility of a quencher to the fluorophore site, a subsequent test evaluated the influence of some water soluble molecules (iodide anions and nitromethane) on the fluorescence of pyrene linked to the COP-B1 (Figure 6). Thus, as can be observed from the Figure 6, a, the addition of KI determines a gradual fluorescence quenching, and for this system the lower quencher concentration for which the fluorescence intensity decreased is of only 0.033 mM KI, while the addition of 1.3 mM KI determined a fluorescence quenching of 79 %. Similarly, the nitromethane molecules induced a fluorescence quenching (Figure 6, b), but in this situation although the detection limit is of only 0.033 mM, the fluorescence intensity diminished at a lower rate, and thus after the addition in the system of 1.1 mM nitromethane the quenching degree is roughly 30 %.

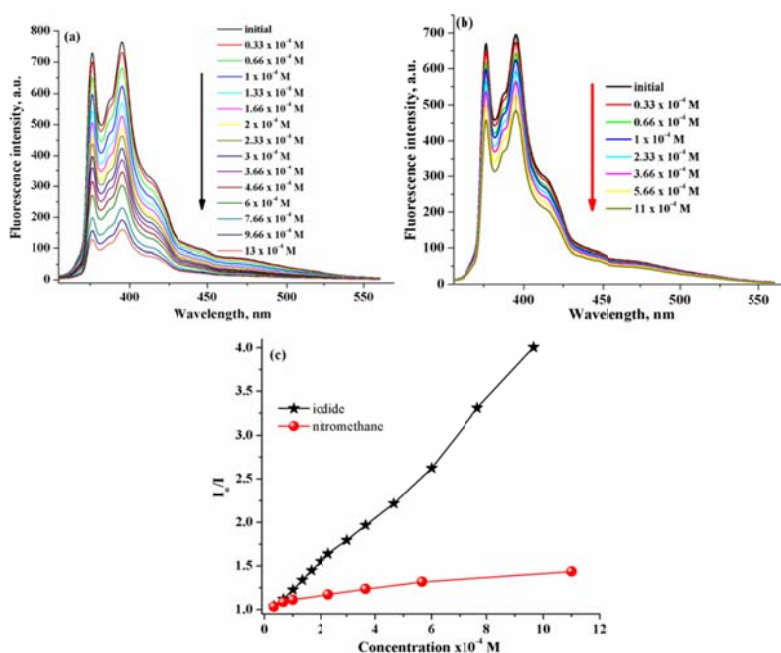


Fig. 6. Fluorescence intensity quenching of COP-B1 in water in the presence of different concentration of KI (a), nitromethane (b) and the Stern-Volmer plots for the quenching (c).

Moreover, comparing the Stern-Volmer plots [36] obtained by the graphical representation of  $I_0/I$  as a function of quencher concentration (Figure 6, c), it can be observed that the  $I_0/I$  ratio increased linearly with iodide quencher concentration with ascending trend to the top, suggesting a facile contact of the quencher molecules with the fluorophore. For nitromethane it seems that  $I_0/I$  plot is not linear and shows a descending curvature generally attributed to the slow quenching process which allow the occurrence of some secondary effects.

Analyzing then the interaction of potassium iodide with thin films based on block copolymers, fundamentally different fluorescence behaviour was observed. Therefore, the fluorescence emission spectra for the polymer films were measured before and after their immersion into solutions containing  $1 \times 10^{-4}$  mole KI, observing that the fluorescence intensity increased with the immersion time (Fig. 7).

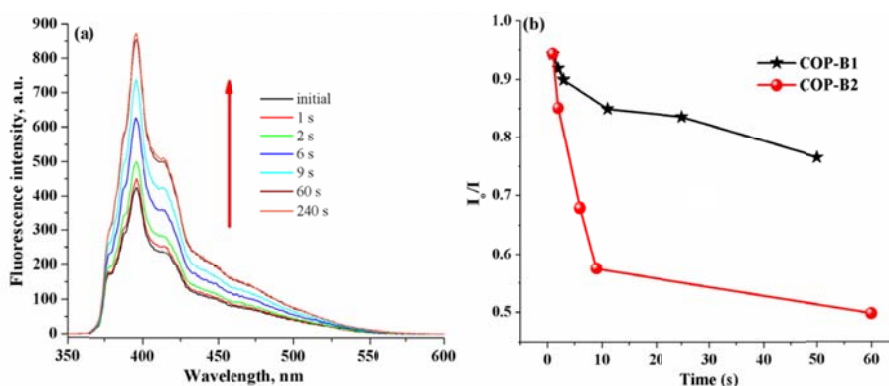


Fig. 7. Fluorescence emission spectra of COP-B2 film as a function of immersion time in deionized water containing  $1 \times 10^{-4}$  M KI (a) and Stern-Volmer plots for both copolymers (b).

It is evident that after 240 seconds of exposure of the COP-B2 film at iodide ions, the  $I_0/I$  ratio becomes 0.48, the fluorescence intensity is augmented with about 100 % and consequently, this analyte acts rather as a “dequencher” of pyrene fluorescence. The experimental results achieved by exposing copolymer block films to aqueous solutions of KI sustain a dissimilar fluorescence response, behaviour of further interest in the design of “turn-on” fluorescent chemosensors.

#### 4. Conclusions

In summary, novel poly(ethylene oxide)-*b*-poly(*n*-butyl methacrylate-*co*-2-methacryloyloxyethylcarbamoyloxymethylpyrene) block copolymers were synthesized via ATRP, yielding materials with high molecular weight and narrow molecular weight distribution at high conversion. The pyrene fluorophore covalently attached on the macromolecular chain emits fluorescence of variable intensities as a function of solvent nature (the most intense fluorescence being detected in water), while in aqueous environment, the presence of heavy metal cations induced miscellaneous degrees of fluorescence quenching. The most efficient quenching effect was found for uranyl cations, so the block copolymer can act as a fluorescent chemosensor for sensitive detection of these transition metal ions. Moreover, the contact of polymer films with aqueous solutions of KI generates an increase of the fluorescence intensity, characteristic exploitable in “turn-on” sensing devices.

#### Acknowledgements

The authors (T.B. and V. M.) gratefully acknowledged the financial support of the European Social Fund - “Cristofor I. Simionescu” Postdoctoral Fellowship Programme (IDPOSDRU/89/1.5/S/55216), Sectorial Operational Programme Human Resources Development 2007 – 2013.

## References

- [1] J. K. Kim, S. Y. Yang, Y. Lee, Y. Kim, *Progr. Polym. Sci.* **35**, 1325 (2010).
- [2] S. B. Darling, *Progr. Polym. Sci.* **32**, 1152 (2007).
- [3] K. M. Ho, W. Y. Li, C. H. Wong, P. Li, *Colloid Polym. Sci.* **288**, 1503 (2010).
- [4] A. Harada, K. Kataoka, *Progr. Polym. Sci.* **31**, 949 (2006).
- [5] Y. Bae, K. Kataoka, *Adv. Drug Delivery Rev.* **61**, 768 (2009).
- [6] K. Skrabania, A. Laschewsky, H. Berlepsch, C. B. Ottcher, *Langmuir* **25**, 7594 (2009).
- [7] W. Li, K. Matyjaszewski, K. Albrecht, M. Moller, *Macromolecules* **42**, 8228 (2009).
- [8] G. Quattrociochi, I. Francolini, A. Martinelli, L. D'Ilario, A. Piozzi, *Polym. Int.* **59**, 1052 (2010).
- [9] K. Demirelli, E. Kaya, M. Coskun, *J. Appl. Polym. Sci.* **99**, 3344 (2006).
- [10] T. J. V. Prazeres, M. Beija, M.-T. Charreyre, J. P. S. Farinha, J. M. G. Martinho, *Polymer* **51**, 355 (2010).
- [11] T. R. Nogueira, M. C. Gonçalves, L. M. F. Lona, E. Vivaldo-Lima, N. McManus, A. Penlidis, *Adv. Polym. Technol.* **29**, 11 (2010).
- [12] N. H. Nguyen, V. Percec, *J. Polym. Sci. Part A: Polym. Chem.* **49**, 4756 (2011).
- [13] W. Zhang, W. Zhang, Z. Cheng, N. Zhou, J. Zhu, Z. Zhang, G. Chen, X. Zhu, *Macromolecules* **44**, 3366 (2011).
- [14] M. J. Nasrullah, A. Vora, D. C. Webster, *Macromol. Chem. Phys.* **212**, 539 (2011).
- [15] A. Krieg, C. Pietsch, A. Baumgaertel, M. D. Hager, C. Remzi Becer, U. S. Schubert, *Polym. Chem.* **1**, 1669 (2010).
- [16] J. S. Wang, K. Matyjaszewski, *J. Am. Chem. Soc.* **117**, 5614 (1995).
- [17] M. Kato, M. Kamigaito, M. Sawamoto, T. Higashimura, *Macromolecules*, **28**, 1721 (1995).
- [18] T. Ozturk, S. Savaskan Yilmaz, B. Hazer, Y. Z. Menceloglu, *J. Polym. Sci. Part A: Polym. Chem.* **48**, 1364 (2010).
- [19] H. Wang, Q. Tao, J. Wang, E. Khoshdel, *Polym. Int.* **60**, 798 (2011).
- [20] M. A. Tasdelen, M. U. Kahveci, Y. Yagci, *Progr. Polym. Sci.* **36**, 455 (2011).
- [21] M. Ouchi, T. Terashima, M. Sawamoto, *Chem. Rev.* **109**, 4963 (2009).
- [22] D. Pestov, C.-C. Chen, J. D. Nelson, J. E. Anderson, G. Tepper, *Sensor Actuator B Chem.* **138**, 134 (2009).
- [23] B.-Y. Wang, X.-Y. Liu, Y.-L. Hu, Z.-X. Su, *Polym. Int.* **58**, 703 (2009).
- [24] L. D. C. Baldi, E. T. Iamazaki, T. D. Z. Atvars, *Dyes Pigments* **76**, 669 (2008).
- [25] M. Mullner, A. Schallon, A. Walther, R. Freitag, A. H. E. Muller, *Biomacromolecules* **11**, 390 (2010).
- [26] D. Altschuh, S. Oncul, A. P. Demchenko, *J. Mol. Recognit.* **19**, 459 (2006).
- [27] K. Jankova, X. Chen, J. Kops, W. Batsberg, *Macromolecules* **31**, 538 (1998).
- [28] S. N. Bhat, A. Sharma, S. S. Rao, S. V. Bhat, *Ionics* **10**, 139 (2004).
- [29] E. Miller, D. Jóźwik-Styczyńska, *Colloid Polym. Sci.* **285**, 1561 (2007).
- [30] A. F. Olea, P. Silva, I. Fuentes, F. Martínez, D. R. Worrall, *J. Photochem. Photobiol. A: Chem.* **217**, 49 (2011).
- [31] P. Bandyopadhyay, A. K. Ghosh, *J. Phys. Chem. B* **113**, 13462 (2009).
- [32] E. C. Buruiana, A. L. Chibac, T. Buruiana, *J. Photochem. Photobiol. A: Chem.* **213**, 107, (2010).
- [33] V. Melinte, T. Buruiana, D. Tampu, E. C. Buruiana, *Polym. Int.* **60**, 102 (2011).
- [34] K. Nakashima, P. Bahadur, *Adv. Colloid Interface Sci.* **123–126**, 75 (2006).
- [35] J. You, J. A. Yoon, J. Kim, C.-F. Huang, K. Matyjaszewski, E. Kim, *Chem. Mater.* **22**, 4426 (2010).
- [36] J. R. Lakowicz, *Principles of fluorescence spectroscopy*, 3<sup>rd</sup> Edition, Springer, New York, pp. 11 (2006).